Co-funded by the Erasmus+ Programme of the European Union

BIOART
Engineering education for human welfare

PETER ARRAS AND DAVID LUENGO (EDS.)

TEACHING AND SUBJECTS ON BIO-MEDICAL ENGINEERING

APPROACHES AND EXPERIENCES FROM THE BIOART-PROJECT

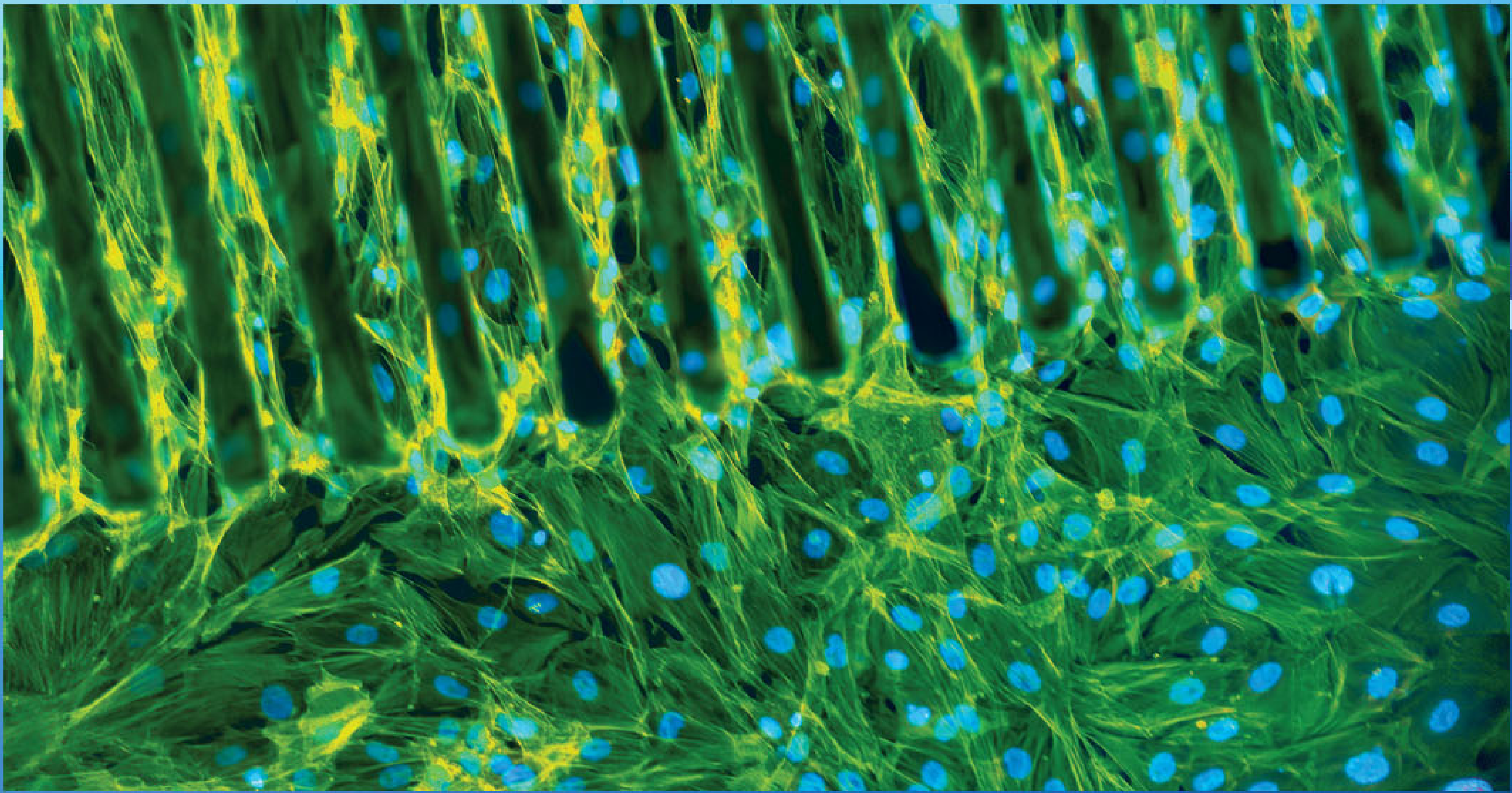

2021

Co-funded by the
Erasmus+ Programme
of the European Union

BIOART
Engineering education
for human welfare

PETER ARRAS AND DAVID LUENGO (EDS.)

TEACHING AND SUBJECTS ON BIO-MEDICAL ENGINEERING

APPROACHES AND EXPERIENCES FROM THE BIOART-PROJECT

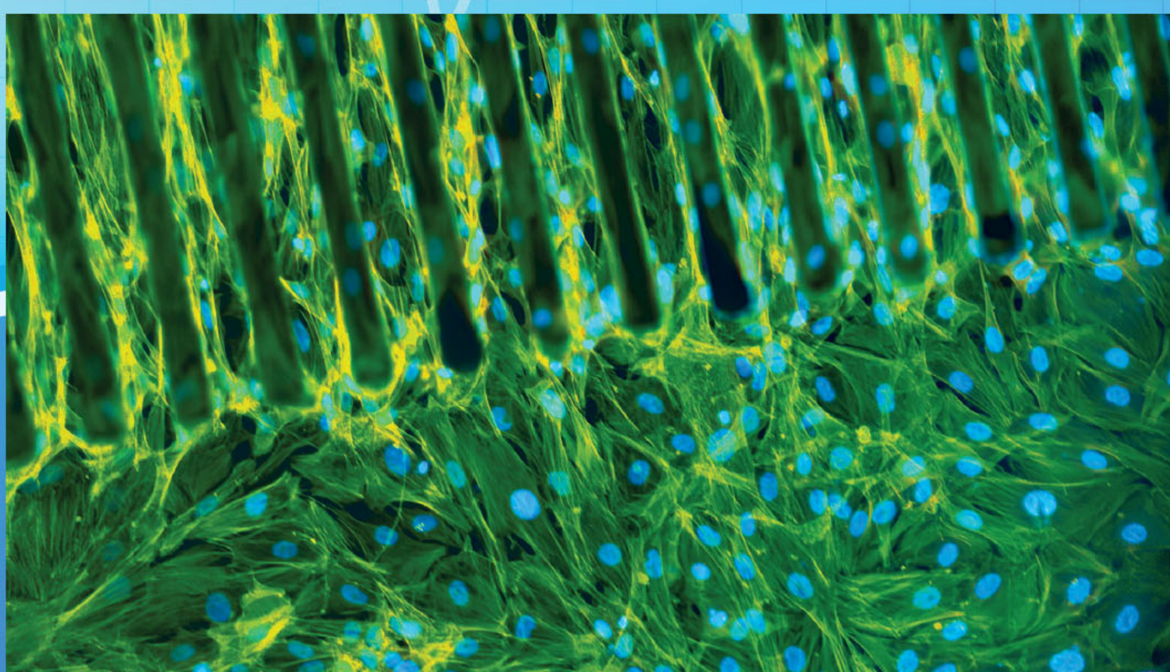

2021

Teaching and subjects on bio-medical engineering

Approaches and experiences from the BIOART-project

Peter Arras and David Luengo (Eds.)

ISBN: 978-94-641-4245-7

Keywords: Bio-medical Engineering, BIOART, implants

Cover Design: Andreiev M.O.

Cover photo: Picture by Rosalba M. Ferraro & Miriam Seiti, AML group KU Leuven in partnership with UniBs: “Cell Culturing on Patterned Substrates for Morphological Stimulation in Neural Tissue Engineering”.

First edition: 2021

The BIOART-project (Innovative Multidisciplinary Curriculum in Artificial Implants for Bio-Engineering BSc/MSc Degrees), 586114-EPP-1-2017-1-ES-EPPKA2-CBHE-JP, has been funded with the support of the Education, Audiovisual and Culture Executive Agency of the European Commission.

Modeling and simulation of prosthetic gait using a 3D model based on perturbation functions

Sergey Vyatkin[1 [0000-0002-1591-3588]], Olexandr Romanyuk[2 [0000-0002-2245-3364]], Yurii Bezsmertnyi[3[0000-0002-1388-7910]], Pavlo Mykhaylov[2 [0000-0001-5861-5970]], Roman Chekhmestruk[2 [0000-0002-5362-8796]]

[1]Institute of Automation and Electrometry, 630090, Novosibirsk, Ak. Koptyuga, 1, Russia
sivser@mail.ru
[2]Politechnika Lubelska, Lublin, Poland
waldemar.wojcik@pollub.pl
[2]Vinnytsia National Technical University, 21021, Vinnytsia, Khmelnytske shose 95, Ukraine
rom8591@gmail.com, psv@vntu.edu.ua
[3]Scientific Research Institute of Invalid Rehabilitation on the base of Vinnytsia Pirogov National Medical University, 21029, Vinnytsia, Khmelnytske shose
104, Ukraine
bezsmertnyiyurii@gmail.com

Abstract. The work describes the method of construction of a lower limb prosthesis, both below and above the knee. It describes the computer-aided design basis and the digital patient model with which the prosthesis is designed and tested in a fully virtual environment. The virtual patient model is the basis of the entire system, using a biomechanical model that takes into account patient characteristics such as anthropometric indicators. The program uses automated and knowledge-based approaches in order to replace the current development process, mainly manual, with a virtual one. A set of tools is used to design, configure and test the prosthesis. Prosthetic modeling allows configuring and generating a three-dimensional model of the prosthesis. The virtual test environment allows the prosthesis to virtually configure the artificial leg and simulate the patient's posture and movements, checking functionality and configuration. A gait model has been developed. For this purpose, the analogy of the double pendulum with the flesh segment of the lower limb was used, which allows to evaluate the gait model as a system using simple final figures or connections. The system representing association of segments is used, the energy exchange between links of the system is analyzed using the Lagrange method. The association analysis is developed by calculating inverse kinematics, which determines the trajectory and position of the system in order to find the forces that carry out this movement and energy transfer. Taken as a

double pendulum, the lower limb has mass and length values based on the weight and height of each part. The obtained values were derived from anthropometric data of the subject.
Keywords: First virtual patient, Lower limb prosthesis, Virtual prototyping, Human modeling, Gait modeling.

1 Introduction

Many information and communications technology tools, such as computer-aided design (CAD) and automated engineering systems, have been developed recently to support the product development process, with the aim of reducing the need for physical prototypes and reducing costs and time. However, the spread of such systems is limited in some areas, especially when the product requires a high level of customization and represents an interface with the human body or its parts. An example would be artificial prostheses, which must be designed according to the shape of a specific anatomical area. This work is emphasized on modular prostheses of the lower limbs, both below the knee (transtibial, TT) and above the knee (transfemoral, TF), realized by assembling modern components in order to obtain maximum comfort and convenience of use [1]. Most of the components are standard, e.g. foot and knee can be selected from the manufacturer's catalogue, while the connection should be implemented based on the patient's anatomy. The connection is the main critical component and is designed and manufactured almost entirely manually, relying heavily on the experience and skills of prosthetic technicians. In addition, the patient plays a key role in the production process, since both standard and specially selected components are selected and projected according to their state of health and anatomical morphology.

Some CAD / CAM prosthetic systems such as Bioshape and Canfit are available on the market. Reverse engineering methods (usually laser scanning) can be used to obtain the external shape of the residual limb from which the connection is made and to modify the basic models stored in libraries. However, they are not integrated with modeling tools such as Finite Element Analysis (FEA) or multi-body systems for checking prosthetic construction. Various works can be found in the literature suggesting that FEA can be used to simulate the behavior of prosthetic components [2-4] and to analyze the interaction between joint and residual limb. Some studies have also demonstrated the feasibility of a fully computer-based connection design process based on the integration of CAD and FEA tools [5], but they are not able to manage all stages of the prosthetic design process in a unique environment and do not provide any assistance to the prosthesis.

This work represents the method of lower limbs prosthetics based on the virtual model of the patient with the use of perturbation functions and theoretical multiple subtraction operation [6]. The main objective was to develop a digital model of an amputated person, which will be used to design and test a prosthesis in a fully virtual environment. In order to achieve the goal of replacing the current process (mainly manual) with a virtual one, several issues were considered: capturing and formalizing the knowledge of orthopedic technicians about this process, obtaining information about the patient and morphology using diagnostic tools, developing comprehensive solutions for designing and testing standard and specially selected components, and using digital methods to simulate the behavior of the prosthesis while walking. The adoption of a digital model to represent the patient is in line with the trend towards multiscale human modeling as a tool for a wide range of applications, from ergonomics to occupational safety and health [7].

The method provides the prosthetic professional with a set of interactive tools for designing, adjusting and testing the prosthesis. It consists of two parts: prosthetic modeling and virtual testing (Fig. 1).

The first part configures and generates a three-dimensional model of the prosthesis, while the second part virtually adjusts the artificial leg and simulates the patient's posture and movements, checking the functionality and configuration of the prosthesis.

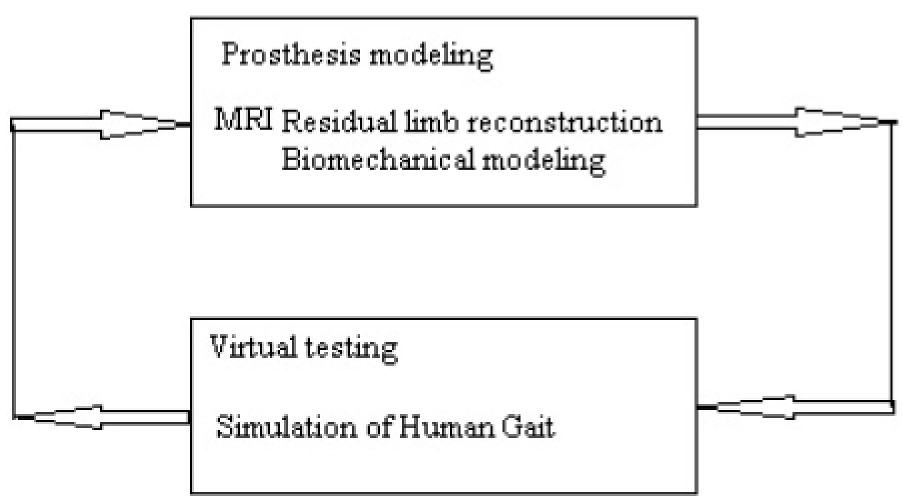

Fig. 1. Virtual patient

MRI is used to scan the patient's leg. Volume data is a three-dimensional array of cubic elements (voxels) representing units of 3D space. At the same time, typical data sets describing physical objects or phenomena are usually represented by files up to several gigabytes in size, since these files contain data about each point of the scanned three-dimensional space. If the interpolated density at the sample point exceeds a certain threshold density, then a density gradient G is calculated from these points *D0,..., D7*, which can be used as a normal to the surface.

An efficient method for converting voxel data arrays into a functional description based on perturbation functions is applied.

Organization

The chapter is organized as follows. Section 2 gives a brief survey of the work related to function representation of objects, rendering and interactive geometric modelling. provides the overview of our approach to computation of the ray-surface intersection. Section 3 describes prosthesis modeling, design of the connection and and configuration of the prosthesis. Virtual testing (the program allows you to set and evaluate the functionality of the prosthesis by simulating the positions and movements of the virtual patient) is presented in Section 4. Analysis of the method described in Section 5. Summary work is discussed in Section 6.

2 Virtual patient

The virtual patient consists of a biomechanical model and a data set. The data are used to adjust the model of the amputated patient. They represent the elements by which the development process is managed, a selection of standard components prior to joining and configuration of the prosthesis. The tasks and decisions made by the prosthetists depend on the characteristics of the patient and their health status. For example, a special kind of foot, identified as a high-energy foot, is suitable for young and healthy patients because it can better maintain high blood pressure. Patient data and information have been grouped into three main categories, namely patient assessment, residual limb assessment and anthropometric indicators.

The first group refers to general patient data, mainly used to select standard components. The second deals with parameters for assessing residual limb condition and creating a three-dimensional joint model. The latter refers to the anthropometric indicators of the patient and the residual limb. They are used for the correct size of the digital patient model, standard components and connection.

The biomechanical model of an amputated person is determined at different levels of detail, depending on the task at hand. For example, compound modeling and simulation require a detailed residual limb model (skin, bone and muscle).

Three main tools are used to create a biomechanical model: a universal human modeling system, medical images of the residual limb (obtained, for example, with MRI or CT) and a special software module for 3D reconstruction of the residual limb.

Perturbation functions are used to create and model the virtual patient [6]. This allows creating a detailed biomechanical model of the human body using rigid links connected through joints to simulate the skeleton and flexible elements to represent muscles, tendons and ligaments. Thus, it is possible to create an individual model modifying anthropometric data. Two reference models were considered, one for amputated TF and one for amputated TT, which should be customized for each individual patient. The following data are needed to characterize the virtual patient: anthropometric patient data and a digital model of the lower limb. This means that the biomechanical model of an amputee is implemented in two stages: the first stage is to determine the model size and the second stage is to determine the residual limb binding [8,9,10].

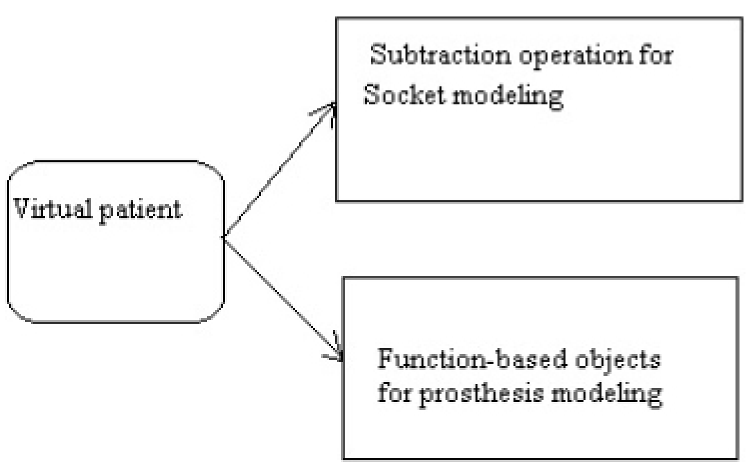

Fig. 2. Prosthesis modeling

2.1 Perturbation functions

Using free forms based on perturbation functions, we model the shape of the prosthesis, using the union operation, we construct the entire prosthesis. Using the subtraction operation, we model the connection socket (Fig. 2). Characteristic feature of a offered method is that the basic primitive things are chosen as surfaces of the second order - quadrics. The quadric is defined by ten coefficients. The same amount of data is necessary for description of a spatial arrangement of one triangular facet. More compact representation of model allows to reduce memory expenses sharply at database storage and, hence, to unload the bus between computing components of system and memory blocks. On the other hand, it is possible to construct smooth objects without defects inherent in polygonal models. On this basis the class of free forms is under construction. It means possibility to describe complex geometrical objects, setting function of deviation from the second order base surface.

The algorithm of recursive multi-level ray-casting (ray-casting) performs an effective search for elements of volume, voxels, involved in the formation of the image. Let us deal with some object representing a three-dimensional scene, which has the property to respond to the request for intersection with a rectangular parallelepiped, or bar. And a negative answer guarantees that this object has no common points with the bar, and a positive answer implies that possibly common points exist. Only the object's functional abilities are important for the algorithm's work, and we won't concretize its internal structure yet. Let's introduce the coordinate system as shown in Figure 3. The search for voxels is done in the space inside the cube, from -1 to 1 for each coordinate, so that the center of the cube corresponds to the origin of the coordinates. At each step of the recursion, the initial volume is broken down into four bars in the x0y screen plane. For each bar, the object is queried to determine the intersection. If the result is positive, the bar is subjected to the next level of recursion. And the bars that gave a negative result of the test for an intersection with the object are not subject to further immersion in recursion, which corresponds to an exception from the consideration of square areas of the screen, on which the bar (and therefore the surface of the object) is not displayed [11,13].

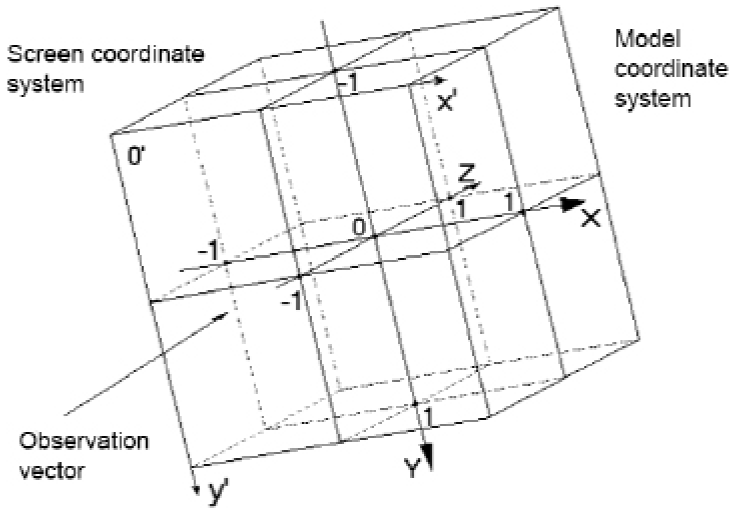

Fig. 3. Unit cube

This stage of the algorithm's work is well illustrated in Fig. 4, where there are empty squares and there are areas of the image not involved in the formation of the image. At a certain step of subdivision we reach bars that are displayed exactly in one virtual pixel of the image. Now we should start subdivision of "thin" bars, rays, along the Z-axis, first performing the request to intersect with the nearest half of the ray. Thus, for each ray at the final level of recursion we will define a voxel containing the surface of the object and closest to the observer. In other words, while searching for volume elements, voxels containing the areas of the object surface forming the image, the given algorithm bypasses the cubic space along the quad tree whose leaves are the roots of binary subtrees [14,15,16].

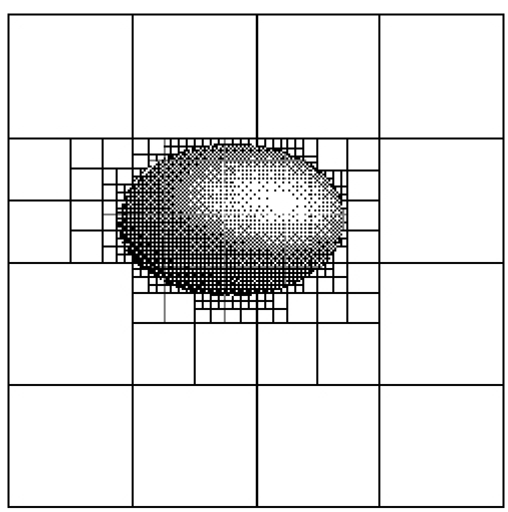

Fig. 4. Quadtree subdivision

The object-square is the basis for building all other objects. The surface forming it is a zero level surface o the square three-dimensional function, i.e. the function of its surface is set implicitly and is defined by ten coefficients (*A*,*B*,*C*,...*K*):

$$Q\ (x\ y\ z) = Ax^2 + By^2 + Cz^2 + Dxy + \\ + Exy + Fyz + Gx + Hy + Iz + K = 0 \quad (1)$$

where *x, y* and *z* are spatial variables. You can write this equation in a matrix form:

$$(x, y, z, 1)\begin{pmatrix} A & D/2 & E/2 & G/2 \\ D/2 & B & F/2 & H/2 \\ E/2 & F/2 & C & I/2 \\ G/2 & H/2 & I/2 & K \end{pmatrix}\begin{pmatrix} x \\ y \\ z \\ 1 \end{pmatrix} = 0 \quad (2)$$

We agree to further call the space in which the algorithm performs the division of cubic volume, working or model and mark it with the letter M. Now let's enter the coordinate system directly related to the real space metric (camera or eye coordinate system). Let's allocate in this space the volume limited by the quadrilateral truncated pyramid, or in other words, the visibility pyramid, which is characterized by depth and angle of field of view (Fig. 5). Let us call this space pyramidal and denote it by the letter P [17,18,19].

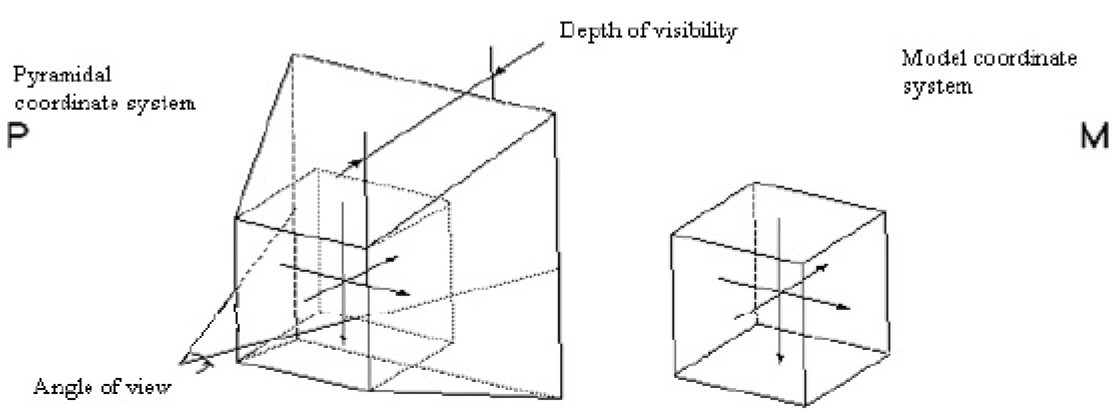

Fig. 5. Visibility pyramid

If the geometrical transformation is described by matrix (C), then the new transformed matrix of coefficients (Q) = $(C)^T$ (Q)(C) operates in space M accordingly to matrix (Q) in space P. In particular, at the stage of space division into a quadric tree, where the compression is performed twice and the transfer to the ± 1 on two coordinates, the recursive transformation of quadric coefficients looks like this:

$$A' = A/4;$$

$$B' = B/4;$$

$$C' = C;$$

$$D' = D/4;$$

$$E' = E/2;$$

$$F' = F/2;$$

$$G' = G/2 + i*A/2 + j*D/4;$$

$$H' = H//2 + i*D/4 + j*B/2;$$

$$I' = I + i*E/2 + j*F/2;$$

$$K' = K + i*G/4 + j*H/4;$$

$$K'' = K' + i*G'/2 + j*H'/2 \quad (3)$$

where the odds without a stroke are taken from the previous step of recursion; variables $i,j = \pm 1$ are determined by the algorithm depending on the direction of immersion in recursion (i - in x axis, j - in y axis). The obtained coefficients are used in the intersection test.

If in the equation of the quadric $Q(x, y, z) = 0$ the values of the variables x, y, z change within the interval [-1, 1], then

$\max[|Q(x, y, z) - K|] \leq$

$\max F = |A|+|B|+|C|+|D|+|E|+|G|+|H|+|I|$; (4)

Now note that if $|K|$ £ $\max[|Q(x, y, z) - K|] \leq \max F$, then perhaps there is a point $M_0 = (x_0, y_0, z_0)$ $(-1 < x_0, y_0, z_0 < 1)$ such that $Q(x_0, y_0, z_0) = 0$. In case $\max F < |K|$, there are no such points, and the sign of the coefficient K

distinguishes the position of the bar inside or outside from the surface of the square $Q = 0$. Based on the results of this test, the algorithm continues to separate only the bars that lie inside the quadric as a whole or, possibly, in part, rejecting deliberately external bars.
The described algorithm displays only the parts of objects that have entered the space inside the cube. The application of projective transformation generalizes the given algorithm into pyramidal volumes, which allows synthesizing images with perspective.

The branch of geometrical knowledge that studies the projective properties of figures is called projective geometry, where homogeneous coordinates are entered to determine the metric in space. In three-dimensional space the point with Cartesian coordinates (x, y, z) corresponds to an infinite set of homogeneous coordinates (x', y', z', a) such that $x = x' / a$, $y = y' / a$, i.e. identical coordinates are determined to the total non-zero multiplier. Of interest is the transformation matrix acting on homogeneous coordinates as follows:

$$\begin{pmatrix} C11 & C12 & C13 & C14 \\ C21 & C22 & C23 & C24 \\ C31 & C32 & C33 & C34 \\ C41 & C42 & C43 & C44 \end{pmatrix} \begin{pmatrix} x_m \\ y_m \\ z_m \\ 1 \end{pmatrix} = \begin{pmatrix} x_p \\ y_p \\ z_p \\ a_p \end{pmatrix}, \text{ or } \quad (C)(M) = (P), \quad (5) \qquad (5)$$

where (C) is the transformation matrix, (M) is the homogeneous coordinates of the space point M, and (P) is the display coordinates in P.

Within the limits of projective geometry the theorem [8,§108] that projective display of space M on space P is unequivocally proved is defined by the task of five pairs of points corresponding on display, provided that from five points set in space M, any four do not lie in one plane. We select five pairs of such reference points (M^i) and (P^i) (the upper index corresponds to the number of a pair) and make a system of equations:

$$(C)(M^i) = r^i (P^i), \qquad (6)$$

where $i = [1..5], r^1, r^2, r^3 r^4$ - unknown multipliers, but $r^5 = 1$. Solving these equations we find the coefficients of the projective transformation matrix

(C), which is further used to transform the geometric primitives.

The free forms are one more wide class of geometric model objects. The surface of the quadrica is a constant level surface of the second order function. $Q(x,y,z)$. Let's define a certain perturbation function, $R(x,y,z)$, which has the property of smoothness.

Now let's consider the function $Q'(x,y,z) = Q(x,y,z) + R(x,y,z)$. Due to its smoothness R and Q Q' it will retain this property and therefore the surface of the zero level will also be smooth. Thus, we have built a complex surface using the second order function as the base. But in order to get the necessary shape of the surface, we must learn to set the corresponding perturbation function in an acceptable way. Smooth perturbation is constructed from a square function as follows. Let's define the inner area Q as part of the space where $0 < Q$. Then in the outer part of Q we put R equal to zero, and in the inner part we erect Q into a cube:

$$R_i(x,y,z) = \begin{cases} Q_i^3(x,y,z), if\ Q_i(x,y,z) \geq 0, \\ 0, if\ Q_i(x,y,z) < 0 \end{cases} \tag{7}$$

We got the function R, which is naturally calculated in the process of recursive subdivision, so that the quad can act as an outrage to other objects. And the object, which we call free form, remains a quadric in its essence but takes into account the additive introduced by the perturbation to its own basic function (Fig. 6). In turn, the free form can be a perturbation function for some other object. Because max $[Q + R] \leq$ max $[Q]$ max $[R]$, it means that to estimate the maximum Q on some interval it is necessary to calculate the maximum of the perturbation function on the same interval.

Fig. 6. Free form

The calculation of all components of pixel color is performed similarly to the following formulas:

$$C = (Q_{ambi}C_{ambi} + Q_{diff}C_{diff} + Q_{spec}C_{spec})/(Q_{ambi} + Q_{diff} + Q_{spec}), \quad (8)$$

where the index "ambi" refers to the characteristics of scattered radiation, and "diff" and "spec" refer to the diffuse and mirror parts of reflected light respectively; C - color components; Q - weighting factors.
Calculations of color components are made on the basis of vector model of illumination [9, Chapt.5]. Four vectors are involved in calculations: normal to surface (n), vector to illumination source (l), direction of reflected light (r) and vector to observer (v):

$$C_{diff}(n,1)C_{lite}C_{surf}; \quad (9)$$

where C_{lite} - source color, C_{surf} - surface color.

$$C_{spec} = (r,v)^p C_{lite}; \quad (10)$$

where p - surface roughness coefficient.

To create a complex scene, it is necessary to describe in it some certain quantity of the primitives necessary for a concrete problem. Displayed object, with which the rasterization algorithm interacts by means of queries, is the whole three-dimensional scene. Therefore the geometrical model should allow to construct objects and their compositions of unlimited complexity (Fig. 7.).

It is reached first of all by application of Boolean operations of association and intersection. All scene represents a kind of a tree which each knot is the object-designer who is carrying out logic operations over the descendants, and tree tops are the primitive things used by system. At the moment when the rastering algorithm addresses any query to the constructor object, this object addresses to the descendants, transforms the received result, and gives the corresponding answer to query. In this case, the descendant can be a primitive, or another object-constructor. At application of geometrical operations, turns, movings, scaling, to the object-designer, it makes all these operations with the descendants [20,21,22,23].

Fig. 7. Combining the three free forms

To create a "connection" in free form, a multiple theoretic subtraction operation is applied (Fig. 8).

$$F(x, y, z) = F_1(x, y, z) \setminus F_2(x, y, z) \quad (11)$$

Deducted residual limb volume from free form

$$G_3 = F_i\,(G_1\ G_2 \qquad (12)$$

where

$$G : f_1\,(x, y, z) \geq 0\ G_2 : f_2\,(x, y, z) \geq 0 \qquad (13)$$

Fig. 8. Free form and "connection".

Using function-based object and subtraction operation, the prosthetic can model the socket emulating the traditional procedures carried out during socket manufacturing (Fig. 9).

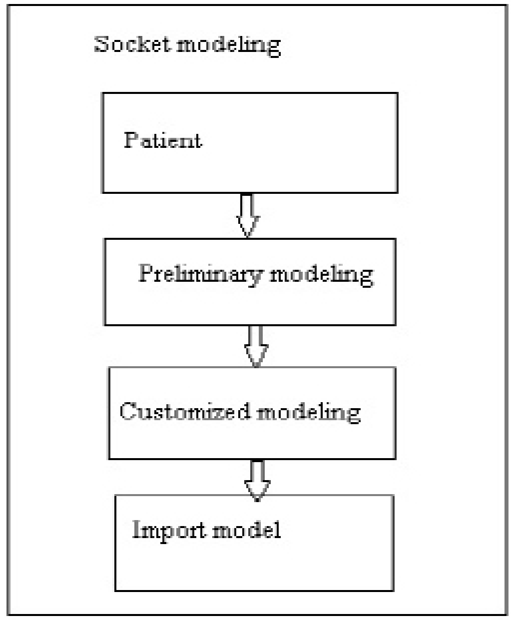

Fig. 9. Virtual socket modeling

2.2 Model size

The correct size of the virtual patient is a key factor in fitting the prosthesis. This means that the anthropometric data of the patient is needed. A distinction is made between general patient data to determine the correct size for the patient and residual limb measurements to position and link the prosthesis to the patient.

Some of these are included or can be derived from the above patient characteristics. Some examples are the hip joint (HJ) and knee joint (KJ), height, weight, and length of the amputated foot. Others, such as shoulder height, can be obtained using a motion capture system.

Once the necessary data has been entered or automatically obtained, the program automatically applies the first level of setting to the virtual patient generating the skeleton, mass, joints and soft tissue based on anthropometric measurements.

2.3 Residual limb attachment

A virtual patient configured with anthropometric data does not include the residual limb relevant for prosthetic design and gait analysis simulation.

A detailed model of the residual limb, including external (skin) and internal (muscles and bones) parts, is based on medical images obtained with an MRI. MRI is preferable to CT because it is less invasive for the patient. However, the end users of the program are podiatrists who do not have special competences and skills in the field of automated tools (for example, tools for medical image processing). Therefore, a software module has been implemented that automatically reconstructs a three-dimensional model of the residual limb without requiring human intervention, starting with the MRI volume [10]. The implemented algorithm first converts the MRI scan into a three-dimensional graph, where the nodes correspond to voxels, and the ribs have weights representing the similarity of neighbors. Aggregate clustering is then performed using features such as intensity and dispersion in regions. Once the graph is segmented in different regions, the algorithm highlights internal bone voxels by analyzing size and shape. The outer surface corresponding to the cult is obtained by a threshold operation. Ultimately, clusters belonging to bones and cult are automatically converted to functional surfaces. The end result is a three-dimensional geometric model, which allows the exchange of CAD information between the program modules.
The residual limb model is imported and linked to the amputated model in two stages:
- The bone segment is first connected to the virtual femur (VF), or to the knee (KJ), using the height of the hip joint and knee joint respectively;
- The residual soft tissue of the limb is then positioned accordingly.
Once an individual virtual patient has been created, the designer can start designing a prosthesis based on the biomechanical model and patient characteristics.

3 Prosthesis modeling

The modeling allows the creation of a three-dimensional model of the prosthesis, which is crucial for the practical study of the installation of the prosthesis and walking of the patient. The modeling and selection of standard and specially selected components is based on the digital layout of the respective anatomical area, the characteristics of the patient (e.g. anthropometric data) and the level of use of the prosthesis. It integrates three basic modules:
- Simulations of the connection (2.1.6).

- A finite element simulation program to analyze the interaction between the stump and the "compound".

3.1 Design of the "connection"

The first two modules are combined, the interface is implemented using an object-oriented language C++.
Using the simulation program, a "connection" (2.1.6) can be created in the denture by simulating the traditional procedures performed during fabrication of the "connection". It is controlled either automatically or semi-automatically and includes a set of design rules derived from the analysis of the traditional process, such as where and how to change the shape of the "connection" or automatically determine the thickness of the "connection" based on the patient characteristics.
Four main stages of the controlled simulation procedure are implemented: patient history, pre-modeling, individual simulation, and final simulation of the "connection" on which other specific modifications will be applied to achieve functional form. The main operations at this stage are performed almost entirely automatically according to the patient's characteristics and the traditional process.
In the next step, the model "connection" is formed directly on the digital residual limb model to be perfectly adjusted to the anatomy of each individual patient. The program provides interactive tools [11] that allow emulating tasks traditionally performed by a technician. It starts to change specific zones by simulating the operations of adding and removing layers. For this purpose, these areas are divided into two categories:
- Loading areas where there are no bone protrusions or tendons and it is necessary to squeeze the "joint" closer to the limb and create pressure to withstand the body weight.
- Unloading zones, where there are no bone protrusions or tendons and the "joint" should not press on the limb and at the same time should not be too wide, because it can cause other physical problems.
The program also offers the correct percentage of material to be added or removed according to the "tone parameter". The designer can decide to automatically apply the values calculated by the program or change the shape with a virtual tool [11]. It is an interactive deformation tool that allows to perform operations of adding and removing material, as the technician

manipulates the plaster cast to be emulated. For example, in the unloading zones the technician adds material from the plaster cast, because the "connection" should not press on the stump and can be quite loose, while in the loading zones the material should be removed to have a tight "connection".

As for the amount of material to be added or removed, eight levels of manipulation with a thickness between 1 and 8 mm are highlighted, which correlate with the stump tone. Finally, the designer forms the top edge automatically or semi-automatically and the program offers the final thickness of the "connection". As a rule, the prosthesis determines the thickness empirically based on the weight of the patient. The following formula is used in the program:

$$S_t = \frac{P_w}{20} \quad , \qquad (14)$$

where S_t - joint thickness (mm), P_w - patient's weight (kg).

A more sophisticated algorithm based on engineering knowledge and mechanical properties of materials can replace this formula.

After modeling a "compound", a simulation is automatically performed to analyze the pressure distribution, which is considered the most important evaluation parameter. Consideration is given to the pain threshold (minimum pressure that causes pain) and pain tolerance (maximum tolerable pressure) for the most important zones [12].

Some modeling assumptions and rules have been adopted:

- Residual limb geometry and "connection". Bones and soft tissues are combined to create a unique piece without geometrical breaks.
- Characteristics of the material. The mechanical properties of joint, bone and residual limb are considered linear, homogeneous and isotropic.
- Boundary conditions and loads. The upper surface of the residual limb is limited. In the first two stages of the analysis no external load is applied, while in the last stage the weight of the amputee is applied to the center of mass of the "connection" in a vertical direction. The movement of the "coupling" and the static constant load are applied gradually in the analysis stages. The interaction between the stumps and the "connection" is simulated using an automated surface-to-surface contact algorithm [13].

- The stages of analysis. The simulation is carried out in three stages: application of the residual limb with prestressing on the residual limb, the adjustment phase to achieve better movement of the "connection" around the residual limb and to achieve maximum comfort, and application of a constant static load (amputated weight).
The program extracts the input analysis from the patient parameters (e.g. patient weight and residual limb length), frees up the files needed to generate the FE model, and selects the scenario (language-specific C++) for analysis. The FE model is created automatically without human intervention. The prosthetist cannot change the characteristics of the FE model, but if necessary, the program allows you to set some parameters, such as material properties. The program then provides analysis and generates an output file containing pressure values that are imported and visualized. The program evaluates the pressure distribution and highlights the zones to be changed using interactive tools. The program then performs the simulation again until satisfactory results are achieved.

3.2 Selection of standard components and configuration of the prosthesis

A special program is used to select standard components and create the final assembly of the prosthesis. The prosthesis program selects the most appropriate standard components for the individual patient and the program offers possible configurations of the entire prosthesis according to the characteristics of the patient.
To simulate a prosthesis, the lower limb prosthesis is divided into modules as follows:
- Connection module: includes inlay, connection and adapters.
- Double adapter: Includes double male or female pyramidal adapters that connect the "joint" and knee in the TF denture and can replace the support in both the TT and TF dentures.
- Knee module (TF amputated only): includes knee prostheses and knee adapters.
- Tube module: includes a connecting pylon and tube adapters.
- Foot module: includes a foot prosthesis, leg adapters and a heel, also called a "virtual heel". Two key issues were considered: component

modelling/calibration and component selection.
Calibration and selection rules were extrapolated from commercial catalogues provided by the main prosthetic brands. Since our goal is to correctly assemble and validate the virtual prosthesis and perform virtual gait analysis, a library was developed containing three-dimensional parametric models for each module. Only those characteristics that affect static and dynamic behavior such as joint weight and position are considered, not the actual shape and appearance of the components. The reference dimensions were taken from real and commercial catalogues. Particular attention was paid to the foot and knee as they are standard components responsible for the behaviour of the entire prosthesis and their selection is a key factor in achieving a satisfactory configuration. There is a huge variety of components on the market, and each manufacturer has its own model. For this reason, instead of taking into account specific models that are subject to frequent variations, a set of stable categories has been identified. As an example for a patient with a TF reputation, the main knee joint typologies have been grouped as follows:

- Fixed: knee with locked center of rotation during walking, which can be unlocked manually if necessary.
- Monocentric: elbows with one centre of rotation, separated for self-braking, friction, pneumatic and hydraulic operation.
- Polycentric: knees with a large number of rotation centres are also divided into selfbraking, friction, pneumatic and hydraulic modes.

To select the right components, two setting procedures (one for TT and one for TF) and a database to automatically select the right components for each type of amputated limb and their respective size.
The program automatically collects all possible combinations of different selected parts and provides the specialist with all relevant specifications. The user can select the most suitable one or modify some components according to the patient's needs. When assembling the components, the system ensures that the alignment of the prosthesis is similar to the skeletal structure of the other leg. Traditionally, this operation is called plumb alignment [24,25,26].

4 Virtual testing

The program allows you to set and evaluate the functionality of the prosthesis by simulating the positions and movements of the virtual patient using the method [14].
First of all, the virtual patient must wear the assembled prosthesis. This is imported from the virtual simulation program and correct positioning is obtained with regard to the prosthesis height and the rotation of the foot relative to the vertical line. In particular, the prosthetic leg must be aligned with the other and the "joint" must fully support the residual limb.
The amputated virtual patient can then be used to perform static alignment and gait analysis during various activities. The basic idea is to provide the prosthetist with a movement law library specialized for patients wearing a prosthesis. This requires learning several movements and poses of the patient during typical daily activities and then deriving the laws of movement for the artificial jointsc [27].
This approach was tested using a motion capture system without markers to determine the laws of motion pertaining to the patient's joint. A data collection program consisting of the following components is used: four cameras, resolution 640 × 480 pixels at 60 Hz, markerless motion capture, computer with processor Intel Core2 CPU E8400 3.0 GHz, and a graphic accelerator GeForce 8800 GTX.
The decision taken is inexpensive and does not require the patient to wear markers because it is based on image and silhouette analysis [15]. It automatically recognizes the different segments of the body and then calculates the position and orientation in three-dimensional space. In this environment, the patient must perform typical daily activities such as walking, sitting, walking up/down, and so on. Obviously, the accuracy of the tracking data is crucial, and the quality of the webcam solution is tested.
In order to replicate the movement with the virtual patient, two issues need to be considered: data conversion and display of the received data on the virtual patient defined in the previous step. Two software modules have been developed that perform these tasks automatically.
In order to achieve accurate simulation of muscle and joint movement, reverse dynamic simulation is first performed to record angles and muscle contraction history for the target body segments (links). "Movement agents are located on the model to control movement and 'teach' joints and soft tissues how to move. In our case, in order to reproduce the functionality of the residual limb, we introduced "augmented movement agents" associated

with the prosthetic segments: three associated with the prosthetic leg, one with a tube below the knee representing the lower part of the leg, one with the knee (for TF) and one with a "connection". Once the movements have been recorded in the reverse dynamic simulation, the compiled movement histories are ready to control the forward dynamic simulation.

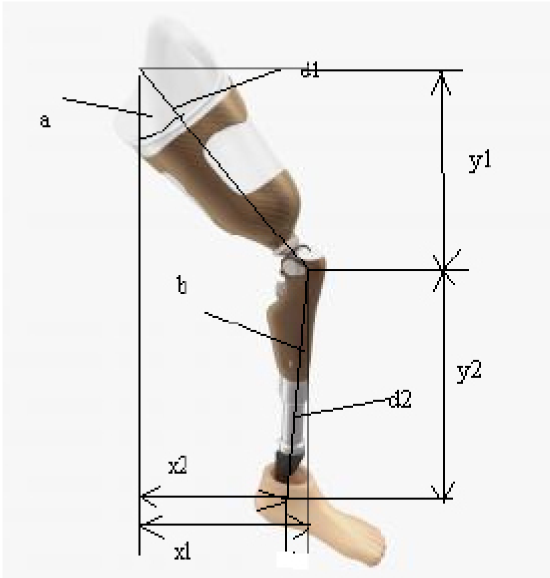

Fig. 10. Lower limb model is set to double pendulum. The lower limb model is used to obtain the gait model. Two compound pendulum segments corresponding to the femur and tibia respectively are considered.

The values d1 and d2 are defined as the lengths of the femur and tibia (Fig. 10). The femur corresponds to the femur segment and the tibia to the leg segment. The position of the femur corresponds to the x and y coordinates in the equations.

$$x_1 = d_1 \sin \alpha \tag{15}$$

$$y_1 = d_1 \cos \alpha \tag{16}$$

The task is to find the energy relations of the system, and for this purpose it is necessary to determine the components of position, speed and acceleration. Concluding (15) and (16) with respect to time, the velocity components are obtained as equations (17) and (18).

$$\dot{x}_1 = d_1 \dot{\alpha} \cos \alpha \tag{17}$$

$$\dot{y}_1 = d_1 \dot{\alpha} \sin \alpha \tag{18}$$

The total speed for the femur is equal to the sum of equations (17) and (18), resulting in equation (19).

$$vms^2 = \dot{x}_1^2 + \dot{y}_1^2 = d_1 \dot{\alpha} \cos^2 \alpha + d_1 \dot{\alpha} \sin^2 \alpha = d_1^2 \dot{\alpha}^2 \tag{19}$$

The kinetic energy of the contralateral thigh is determined by the equation (20).

$$E_{k1} = \frac{1}{2} m_1 vms^2 \tag{20}$$

Let's substitute (19) in (20) with the expression for hip kinetic energy, equation (21).

$$E_{k1} = \frac{1}{2} m_1 d_1^2 \dot{\alpha}^2 \tag{21}$$

Equation (22) represents the potential energy for the thigh.

$$E_{p1} = m_1 g y_1 \tag{22}$$

Substitution (16) in (22) gives equation (23), which corresponds to the potential thigh energy.

$$E_{p1} = -m_1 d_1 g \cos \alpha^1 \tag{23}$$

The above described mathematical procedure used for the hip is repeated for the leg. The position of the leg is determined by equations (24) and (25).

$$x_2 = x_1 + d_2 \sin \beta = d_1 \sin \alpha + d_2 \sin \beta \tag{24}$$

$$y_2 = y_1 - d_2 \cos \beta = -d_1 \cos \alpha - d_2 \cos \beta \tag{25}$$

The speed components are determined by equations (26) and (27)

$$\dot{x}_2 = x_1 + d_2 \dot{\beta} \cos\beta = d_1 \dot{\alpha} \cos\alpha + d_2 \dot{\beta} \cos\beta \tag{26}$$

$$\dot{y}_2 = y_1 + d_2 \dot{\beta} \sin\beta = d_1 \dot{\alpha} \sin\alpha + d_2 \dot{\beta} \sin\beta \tag{27}$$

The full speed for the leg is determined by equation (28).

$$vps^2 = \dot{x}_2^{\,2} + \dot{y}_2^{\,2} = (d_1 \dot{\alpha} \cos\alpha + d_2 \dot{\beta} \cos\beta)^2 + + \left(d_1 \dot{\alpha} \sin\alpha + d_2 \dot{\beta} \sin\beta \right)^2 \tag{28}$$

Equation (29) corresponds to kinetic energy for the leg, and equation (30) refers to kinetic energy for the leg.

$$E_{k2} = \frac{1}{2} m_2 vps^2 \tag{29}$$

$$E_{k2} = \frac{1}{2} m_2 (d_1^2 \dot{\alpha}^2 \, d_2^2 \dot{\beta}^2 + 2 d_1 d_2 \dot{\alpha} \dot{\beta} \cos(\alpha - \beta)) \tag{30}$$

Equation (31) describes the potential energy of the leg.

$$E_{p2} = -m_2 \, (d_1 g\cos\alpha + d_2 g\cos\beta) \tag{31}$$

The total kinetic energy of all segments of the body, thigh and tibia is presented in equation (32).

$$E_{kt} = E_{k1} + E_{k2}$$
$$E_{kt} = \frac{1}{2} m_1 d_1^{\,2} \dot{\alpha}^2 + \frac{1}{2} m_2 (d_1^2 \dot{\alpha}^2 \, d_2^2 \dot{\beta}^2 + 2 d_1 d_2 \dot{\alpha} \dot{\beta} \cos(\alpha - \beta)) \tag{32}$$

The total potential energy for the entire lower segment of the facility is shown in equation (33).

$$E_{pt} = E_{p1} + E_{p2} \tag{33}$$

$$E_{pt} = -m_1 d_1 g\cos\alpha - m_2(d_1 g\cos\alpha + d_2 g\cos\beta)$$

After obtaining the final energy values, Lagrangian is calculated in equation (34).

$$L = E_{kt} - E_{pt} \tag{34}$$

Equation (35) is the Lagrangian equation of motion, and equation (36) is for β.

$$\frac{d}{dt}\left(\frac{\partial L}{\partial \dot{\alpha}}\right) - \frac{\partial L}{\partial \alpha} = 0 \tag{35}$$

$$\frac{d}{dt}\left(\frac{\partial L}{\partial \dot{\beta}}\right) - \frac{\partial L}{\partial \beta} = 0 \tag{36}$$

5 Results

A comprehensive program check is quite complex. In addition, it requires the active participation of prosthetics and patients.

At present, the proposed program has been tested in three stages at various levels to gradually test the new design process and the development of automated tools. The first step concerns the prosthetic configuration, the second step concerns the prosthetic simulation process and the last step concerns the entire design process, from simulation to testing.

Testing was done on a computer with a processor Intel Core2 CPU E8400 3.0 GHz, and a graphic accelerator GeForce 8800 GTX.

5.1 Prosthetic Configuration

The goal was to check the validity of the knowledge-based configuration procedures and the selection and calibration rules adopted for standard components. Several amputated TF and TT models were considered [16-18]. Several patients were selected to cover a variation of all parameters. Four parameters required for the selection procedure were collected for each patient: patient weight, lifestyle factors, residual limb length and patient strength. As soon as the data were obtained, the program automatically selected the most appropriate foot and knee prostheses (for TF). The program is designed to facilitate selection by providing a list of the most effective components. This solution is preferable to a single result, as some other factors (e.g. aesthetic or cultural aspects) may influence the final choice. The configurations proposed by the programme have been compared with those identified through the traditional process.

Test cases for which no suitable matches were found were explained by the fact that some patient characteristics could not be quantified. For example, for a middle aged patient who is in good health but not motivated, a less effective prosthesis is preferable because it will be easier to use and shorten training time. Another example concerns the aesthetic aspect of components: Some people may prefer a small component, while the system may choose a larger but more effective component.

5.2 Prosthetic modeling

In this case, the purpose of the experiments was to test the prosthetic modeling approach and the results were mostly qualitative. Two cases were examined: amputated TT, 41 years old, height 173 cm, and TF, 47 years old, height 176 cm.

First, the "connection" was simulated and then the entire prosthesis was adjusted.

The geometry of the residual limbs of both amputated limbs was obtained and reconstructed; then patient data were entered, a three-dimensional model of the "connection" was created according to the procedure and rules proposed by the program, according to the characteristics of the patient. This is particularly important because most operations depend on the patient's characteristics, such as changing critical zones (loading and unloading zones), which significantly affect the shape of the "connection". The main objective was to verify the effectiveness of simulation/strain tools and the feasibility of a knowledge-based approach to designing a product, a "connection", that is precisely tuned and characterized by a strict interaction with the human body.

After model creation of "connection" (Fig. 6) the program automatically starts modeling and visualizes results. The program evaluates the pressure values of the critical areas and offers the necessary modification. The

simulation results for the amputated TT show a uniform and consistent pressure distribution, except for the medial region of the tibia. To reduce the pressure in the medial region of the tibia (the "loading area"), the program automatically changes the geometry of the "connection" in this area and the prosthesis can also change it using virtual tools. The program then performs the simulation again.
The next step was to adjust the entire prosthesis. Based on patient data, the system provides the specialist with the appropriate components and adapters, dimensioning them and assembling all the parts. For example, for a patient with TF, the program automatically offered two types of feet (mono-axial high-energy and multi-axial sandwich feet) and two elbows (mono- and polycentric pneumatic knee). Once the respective components had been confirmed, the program extracted three-dimensional parametric models of the standard components from the database and assembled them together with the "connection" to obtain a virtual prototype of the full denture.
Some modifications are required to facilitate the use of simulation tools, especially for users who do not own a computer. For this purpose, the use of new interaction tools, such as a tactile device, to make simulations of "connections" more natural is evaluated.

5.3 Projecting: from modeling to testing

This test has allowed to check feasibility of all process, from modeling to the virtual approach to testing.
The entire design process was tested for an amputated TF. A virtual patient model with anthropometric indices and residual limb morphology was created. The prosthesis was then configured, simulated and tested. A virtual patient wearing an artificial limb was generated and two typical situations were simulated: patients walk on a flat floor and climb a step.
The preliminary results are considered promising, but further programme improvements are needed.

6 Conclusion

This paper presents virtual patients and a software platform designed to design and configure both TF and TT dentures using only digital models and virtual instruments. The digital patient is the core of the entire program around which the prosthetist designs and tests the virtual prosthesis, following the rules during the development of the proposed product. Experiments were conducted with a variety of test cases and with the involvement of highly specialized orthopaedic clinicians in order to get feedback directly from end users, check the effectiveness and usability of the instruments and check the suitability of the digital patient.

Technical experts evaluated the simulation tools for their ease of use. The configurations offered by the program are consistent with those obtained through traditional procedures, with the advantage that different configurations can be generated and compared more easily. The residual limb model has been found to be adequate either to simulate the connection or to simulate the connection and residual limb interaction. With regard to the latter topic, experimental work will be carried out on the best characteristics of material properties by means of indentation tests and obtaining real values of pressure in critical areas of the human part under consideration to test the given FE model. We also consider the possibility of introducing tactile interaction tools to support the simulation phase of compounds and make the procedure of compounds formation more natural and similar to the traditional one. Preliminary tests were performed using a low-cost haptic device. The results are interesting and a more sophisticated device is planned, taking into account the inexpensive solutions.

The approach to virtual testing and using a digital patient of a real person wearing a prosthetic device is promising, but further development and improvement are needed to make it easily applicable. The proposed program can reduce the number of prototypes and the psychological impact on the patient's life. The automated approach allows for all stages of the traditional "compound" development process.

References

1. Smith D. G., Michael J. W., Bowker J. H. (eds). 2004. Atlas of Amputations and Limb Deficiencies: Surgical, Prosthetic, and Rehabilitation Principles. Rosemont, IL: American Academy of Orthopedic Surgeons.
2. Frillici F. S., Rissone P., Rizzi C., Rotini F. The Role of Simulation Tools to Innovate the Prosthesis Socket Design Process. In Intelligent production machines and systems" (eds D. T. Pham, E. E. Eldukhri, A. J. Soroka), pp. 612–619. 2008. Dunbeath, UK: Whittles Publishing.
3. Dou P., Jia X., Suo S., Wang R., Zhang M. Pressure Ddistribution at the Stump/Socket Interface in Transtibial Amputees During Walking on Stairs, Clinical Biomechanics, Vol: 21, Issue 10. pp. 1067-1073 (2006).

4. Faustini M. C., Neptune R. R., Crawford R. H. The Quasi-Static Response of Compliant Prosthetic Sockets for Transtibial Amputees using Finite Element Methods. Medical Engineering & Physics, Volume 28, Issue 2, pp.114-121(2006).
5. Goh J. C., Lee R. S., Toh S. L., Ooi C. K. Development of an Integrated CAD-FEA Process for Below-Knee Prosthetic Sockets. Clin. Biomech.20, pp. 623–629 (2005).
6. Vyatkin S., Romanyuk A, Nechiporuk M., Romanyuk O., Troianovska T. Visualization of volumetric data and functionally defined surfaces using graphics processing units. CONFERENCE 2019. Big Data Processing: Methods, Models and Information Technologies. Series: Applied Research in Computer Science. pp. 216-228. Edited by Oleg I. Pursky. Shioda GmbH, Steyr, Austria, (2019).
7. McFarlane N. J. B., Lin X., Zhao Y, etc. Visualization and Simulated Surgery of the Left Ventricle in the Virtual Pathological Heart of the Virtual Physiological Human. Interface Focus, Volume 1, Issue 3, pp. 374–383 (2011).
8. Woods F. Higher Geometry. Publisher: Applewood Books, 2012.
9. Rogers D. Algorithmic foundations of computer graphics. Mir, Moscow, 1989.
10. Vyatkin S. I, Romanyuk A. N, Krupoderova L. M. Method of three-dimensional compression of volumetric data. CONFERENCE 2020. Actual problems of science and practice, Abstracts of XIV International Scientific and Practical Conference, Stockholm, Sweden, pp. 290-293 (2016).
11. Vyatkin Sergei. I., Romanyuk Olexander N, Al-Maitah Mohammed, Romanyuk Oksana V, Nykiforova Larysa E, Sawicki Daniel, Demsova Natalia. Function-based interactive editing of decoration and material properties. Proceedings SPIE 10808, Photonics Applications in Astronomy, Communications, Industry, and High-Energy Physics Experiments 2018. Vol. 10808.
12. Lee W. C., Zhang M., Mak A. F. Regional Differences in Pain Threshold and Tolerance of the Transtibial Residual Limb: including the effects of age and interface material. Arch. Phys. Med. Rehabil. 86, pp. 641-649.
13. Vyatkin S. I., Romaniuk O. N., Kyrylashchuk S. A., Nechiporuk M. L. Animation of threedimensional objects using iterative methods. International periodic scientific journal. Modern engineering and innovative technologies. Is. 7, Part 1. - Karlsruhe, Germany. pp.. 59 – 62 (2019).
14. Vyatkin Sergey, Romanyuk Alexander, Romanyuk Oksana, Nechyporuk Mykola, Troyanovskaya Tatiana and Tsikhanovska Olena. Photorealistic object reconstruction using perturbation functions and features of passive stereo projection. CONFERENCE ACIT' (2020).
15. Bezsmertnyi Y.O., Shevchuk V.I., Grushko O.V., Tymchyk S.V., Bezsmertna H.V., Dzierżak R, et al. Information model for the evaluation of the efficiency of osteoplasty performing in case of amputations on below knee. Proc. SPIE 10808, Photonics Applications in Astronomy, Communications, Industry and High-Energy Physics Experiments 2018, 108083H (2018).
16. Shevchuk V.I., Bezsmertnyi Y.O., Kyrychenko V.I. M’iazova plastyka pid chas amputatsii i reamputatsii homilky [Muscular plastic during amputation and abdominal shaft. Orthopedics, traumatology and prosthetics]. Ortopedija, travmatologija i protezirovanie. 4, (2010), pp. 13-18 9 (2010). (in Ukrainian).
17. Shevchuk V.I., Bezsmertnyi Y.O., Maiko V.M. Kistkova plastyka pry amputatsiiakh ta reamputatsiiakh nyzhnikh kintsivok [Bone plastics with amputations and reamputs of the lower extremities]. Ortopedija, travmatologija i protezirovanie. 1, (2011), pp 47-55 (2011). (in Ukrainian).
18. Yurii O. Bezsmertnyi, Viktor I. Shevchuk, Sergii V. Pavlov, "Prognosis of efficacy of medical and social rehabilitation in disabled individuals with respiratory diseases", Proc. SPIE 11176, Photonics Applications in Astronomy, Communications, Industry, and High-Energy Physics Experiments 2019, 1117633 (6 November 2019); https://doi.org/10.1117/12.2537340.

19. Yurii O. Bezsmertnyi, Sergii V. Pavlov, and etc. "Information model for forecasting of violation reparative osteogenesis of long bonds", Proc. SPIE 11176, Photonics Applications in Astronomy, Communications, Industry, and High-Energy Physics Experiments 2019, 111762A (6 November 2019); https://doi.org/10.1117/12.2536250.
20. Sergey I. Vyatkin, Olexander N. Romanyuk, Sergii V. Pavlov, and etc. "Transformation of polygonal description of objects into functional specification based on three-dimensional patches of free forms", Proc. SPIE 11176, Photonics Applications in Astronomy, Communications, Industry, and High-Energy Physics Experiments 2019, 1117622 (6 November 2019); https://doi.org/10.1117/12.2537043.
21. Sergey I. Vyatkin, Olexander N. Romanyuk, Sergii V. Pavlov, and etc. Offsetting and blending with perturbation functions // Proc. SPIE 11045, Optical Fibers and Their Applications 2018, 110450W, 2019; doi: 10.1117/12.2522353; https://doi.org/10.1117/12.2522353.
22. Sergey I. Vyatkin, Olexander N. Romanyuk, Sergii V. Pavlov, and etc. A GPU-based multivolume rendering for medicine // Proc. SPIE 11045, Optical Fibers and Their Applications 2018, 1104513, 2019); doi: 10.1117/12.2522408.
23. Sergey I. Vyatkin, Olexander N. Romanyuk, Sergii V. Pavlov, and etc. Offsetting and blending with perturbation functions // Proc. SPIE 10808, Photonics Applications in Astronomy, Communications, Industry, and High-Energy Physics Experiments 2018, 108082Y, doi: 10.1117/12.2501694..
24. Sergey I. Vyatkin, Sergii A. Romanyuk, Sergii V. Pavlov, and etc. Using lights in a volumeoriented rendering // Proc. SPIE 10445, Photonics Applications in Astronomy, Communications, Industry, and High Energy Physics Experiments 2017, 104450U; doi: 10.1117/12.2280982..
25. Oleg G. Avrunin; Maksym Y. Tymkovychhttp://profiles.spiedigitallibrary.org/summary.aspx?DOI=10.1117%2f12.22 29040&Name=Sergii+V.+Pavlov; Sergii V. Timchik; Piotr Kisała, et al. Classification of CT-brain slices based on local histograms, *Proc. SPIE* 9816, Optical Fibers and Their Applications 2015, 98161J (December 18, 2015); doi:10.1117/12.2229040.
26. Olexander N. Romanyuk; Sergii V. Pavlov; Olexander V. Melnyk; Sergii O. Romanyuk; Andrzej Smolarz, et al. Method of anti-aliasing with the use of the new pixel model, *Proc. SPIE* 9816, Optical Fibers and Their Applications 2015, 981617 (December 18, 2015); doi:10.1117/12.2229013.
27. S. O. Romanyuk, S. V. Pavlov, O. V. Melnyk. New method to control color intensity for antialiasing. Control and Communications (SIBCON), 2015 International Siberian Conference. - 21-23 May 2015. - DOI**:** 10.1109/SIBCON.2015.7147194.